Study of internal transport barrier triggering mechanism in tokamak plasmas

J.Q. Dong, Z.Z. Mou, and Y.X. Long

Southwestern Institute of Physics, P.O. Box 432, Chengdu, China

S. M. Mahajan

Institute for Fusion Studies, The University of Texas at Austin, Austin, TX 78712, USA

Abstract

The sheared flow layers driven by the magnetic energy, released in tearing-reconnection processes inherent in dissipative magneto-hydrodynamics (MHD), are proposed as a triggering mechanism for the creation of internal transport barrier (ITB) in tokamak plasmas. The double tearing mode, mediated by anomalous electron viscosity in configurations with non-monotonic safety factor, is investigated as an example. Particular emphasis is placed on the formation of sheared poloidal flow layers in the vicinity of the magnetic islands. A quasilinear simulation demonstrates that the sheared flows induced by the mode have desirable characteristics (lying just outside the magnetic islands), and sufficient levels required for ITB formation. A possible explanation is also proffered for the experimental observation that the transport barriers are preferentially formed in the proximity of low order rational surfaces.

The ever present associative connection between internal transport barrier (ITB) formation and the existence of a highly increased sheared flow is highly indicative that either one is the causal of other or both stem from the same triggering mechanism. In this paper we propose and discuss a mechanism, based on the conversion of magnetic energy released in a tearing-reconnection process, which can create rather localized sheared flow layers with characteristics and magnitudes similar to the ones observed in ITB experiments.

ITBs are formed when neutral beam injection (NBI) or radio frequency (RF) heating power is higher than a minimum threshold in tokamak discharges. The minimum power required depends on plasma conditions when the NBI or RF waves are launched. The advanced tokamak (AT) operation with non-monotonic safety factor (q) profile has lower thresholds than plasmas with monotonic q profiles. As a result, the AT mode of operation is highly desirable for a tokamak reactor.

Whereas reduced turbulent transport in the stationary phase after the formation of an ITB can be explained invoking the sheared perpendicular rotation resu1ting from the improved confinement within the ITB itself, the dynamics of the formation of ITB is not yet well understood. The delineation of the physics of ITB triggering mechanism will assist the ultimate goal of active control of the onset, duration and confinement resulting from the formation of ITB in AT plasmas. The required power may also be lowered through adjusting profiles of plasma parameters such as pressure, temperature, velocity and current. Therefore, in recent years, the conditions, especially the radial position, for triggering the formation of an ITB have been intensively investigated in theory and experiment.

A particularly interesting observation is that the ITB's are formed near low order rational flux surfaces (especially, $q = 2$, $5/2$ and 3). It was first reported from JT-60U that the radial position of the ITBs for both ion temperature T_i and plasma toroidal velocity v_ϕ most likely coincides with the $q = 3$ flux surfaces [1]. In DIII-D too the ITB growth events are well correlated with integral q, although there are several counter examples [2]. The "type II" confinement transition in TFTR discharges requires lower NBI power than the threshold for enhanced reverse shear (ERS) transition and often occurs when $q_{\min}$, the value of q at the surface of shear reversal, crosses rational values, $q = 3$ and $5/2$ in particular [3]. In electron

cyclotron heated L mode discharges on the RTP tokamak, the electron temperature (T_e) profile can be well simulated with a thermal diffusivity, χ_e model which has alternating layers of low and high χ_e located near and away from low q rational flux surfaces, respectively [4]. In ASDEX Upgrade reversed shear experiments, the onset of ITB is usually accompanied by MHD activity. In the 80 discharges studied, there is not a single one in which a clear ITB forms without the presence of MHD activity [5]. It was observed in JET experiments that the radial position of ITBs always coincided with the $q = 2$ or $q = 3$ surface in low core magnetic shear discharges. In addition, an appropriate q profile, and in particular the location of the $q = 2$ surface, is essential for triggering of ITBs. With negative central magnetic shear, the analysis of ITB triggering reveals a correlation between the formation of the ITB and $q_{\min}$ reaching an integral value ($q = 2$ or 3). The time of ITB emergence was also found to coincide with the time when $q_{\min}$ reaches 2 [6]. **A comprehensive recent review on ITB in tokamaks, including experiment and theory, is given by Wolf [7].**

The minimum power threshold represents an external condition that must cause required changes in local (at the position of ITB formation) as well as global (profile) plasma and magnetic configuration parameters in order to form an ITB at the position. An increase in the $\boldsymbol{E} \times \boldsymbol{B}$ shear (in the region of ITB formation) has been identified as one of these changes. In addition, it has been shown that a self-organized layer with the features of an ITB may exist in collisionless plasmas. One of the necessary conditions for the formation of such a layer is a poloidal velocity corresponding to a poloidal Mach number of order unity [8]. However, we still have to establish the relevant relationship between the position where such dramatic increase of flow velocity takes place and plasma properties. In other words, the reason that a flow layer emerges and an ITB forms at a specific position and not elsewhere in a discharge has not been addressed in detail. Especially, the observations that the ITBs form preferentially in the proximity of low order rational surfaces has not been satisfactorily explained.

It is well know that low order rational flux surfaces are prone to the excitation of ideal and dissipative MHD instabilities and that magnetic energy released in the development of the modes may drive significant plasma flows. Therefore, besides fishbone oscillations, other MHD instabilities, forming magnetic islands are proposed as plausible triggering mechanisms for the formation of ITBs in the proximity of low order rational surfaces in ASDEX Upgrade reversed shear discharges [5]. External kink modes coupled to inner rational surfaces have

been shown to be able to trigger ITBs in positive shear discharges in JET [6]. However, the double ITB structure observed in JET reversed magnetic shear discharge has not been addressed in detail [9].

The linear double tearing mode mediated by anomalous electron viscosity was studied in Ref. [10] where the possibility for such modes to drive ITBs was also suggested. By simulating the quasi-linear development of this mode, we demonstrate in this paper the creation of sizable sheared poloidal flow layers in the vicinity of the magnetic islands. The nature and magnitude of the generated flows makes the double tearing mode a strong candidate for the triggering of ITBs in tokamak plasmas with non-monotonic q profiles.

We consider a plasma slab of length a in the x-direction, with a current in the z-direction, and zero equilibrium flow velocity $\boldsymbol{V}_0 = 0$ embedded in the standard sheared magnetic field

$$\boldsymbol{B}_0(x) = B_{0y}(x)\widehat{\boldsymbol{y}} + B_{0z}(x)\widehat{\boldsymbol{z}}, \tag{1}$$

where $B_{0y}(x)$ equals zero at $x = \pm x_s$. The stability of this initial configuration will be examined with respect to two-dimensional, incompressible perturbations. The vector fields are expressible in terms of two scalar potentials: the flux function $\psi(x, y, t)$,

$$\boldsymbol{B}_\perp = \nabla\psi \times \widehat{\boldsymbol{z}}, \tag{2}$$

and the stream function $\phi(x, y, t)$,

$$\boldsymbol{V}_\perp = \nabla\phi \times \widehat{\boldsymbol{z}}. \tag{3}$$

With electron viscosity, the Ohm's law becomes

$$\boldsymbol{E} = \eta\boldsymbol{j} - \frac{1}{c}\boldsymbol{V} \times \boldsymbol{B} - \frac{m_e\mu_e}{n_e e^2}\nabla^2\boldsymbol{j}. \tag{4}$$

It is straightforward to write the z-component of Eq. (4) as

$$\frac{\partial\psi}{\partial t} = -\boldsymbol{V}\cdot\nabla\psi + \frac{c^2}{4\pi}\eta\nabla^2\psi - \frac{m_e\mu_e c^2}{4\pi n_e e^2}\nabla^4\psi, \tag{5}$$

after using Eq. (2) and Faraday's law. Here, η is the plasma resistivity, μ_e is the parallel electron viscosity diffusion coefficient, m_e the electron mass, n_e the electron density, and e and c are, respectively, the electron charge and the speed of light. The z-component of the curl of plasma motion equation may be written as

$$\frac{\partial}{\partial t}(\nabla^2\phi) = -(\boldsymbol{V}\cdot\nabla)\nabla^2\phi + \frac{1}{4\pi\rho}\left[\nabla(\nabla^2\psi)\times\nabla\psi\right]\cdot\widehat{\boldsymbol{z}}, \tag{6}$$

where ρ is the mass density of the plasma. Normalizing all lengths to a, time to $\tau_h = a/v_A$, the poloidal Alfvén time of a plasma column of scale width a, and the magnetic field to some standard measure B_0, Eqs. (3), (5), and (6) transform to:

$$\frac{\partial \psi}{\partial t} = \{\phi, \psi\} + \frac{1}{S}\nabla^2\psi - \frac{1}{R}\nabla^4\psi + E', \tag{7}$$

$$\frac{\partial}{\partial t}(\nabla^2\phi) = \{\phi, \nabla^2\phi\} - \{\psi, \nabla^2\psi\}, \tag{8}$$

where $S = \tau_r/\tau_h$ is the magnetic Reynolds number with $\tau_r = 4\pi a^2/c^2\eta$, $R = \tau_v/\tau_h$ is the fluid dynamic Reynolds number, while $\tau_v = 4\pi a^4 n_e e^2/c^2\mu_e m_e = \omega_{pe}^2 a^4/c^2\mu_e$, and

$$\{\phi, \psi\} = \frac{\partial \phi}{\partial x}\frac{\partial \psi}{\partial y} - \frac{\partial \psi}{\partial x}\frac{\partial \phi}{\partial y}$$

is the Poisson bracket. Assuming the perturbation potentials

$$\phi = \sum_{m=1}^{\infty} \overline{\phi}_m(x,t)\sin(mky), \tag{9}$$

and

$$\psi = \delta\psi(x,t) + \sum_{n=1}^{\infty} \overline{\psi}_n(x,t)\cos(nky), \tag{10}$$

we obtain the following coupled quasilinear equations from the first harmonic perturbation,

$$\frac{\partial \delta\psi}{\partial t} = -\frac{k}{2}\left(\frac{\partial \overline{\phi}_1}{\partial x}\overline{\psi}_1 + \overline{\phi}_1\frac{\partial \overline{\psi}_1}{\partial x}\right) + \frac{1}{S}\left(\frac{d^2\psi_0}{dx^2} + \frac{\partial^2\delta\psi}{\partial x^2}\right) - \frac{1}{R}\left(\frac{d^4\psi_0}{dx^4} + \frac{\partial^4\delta\psi}{\partial x^4}\right) + E' \tag{11}$$

$$\frac{\partial \overline{\psi}_1}{\partial t} = -k\overline{\phi}_1\left(\frac{d\psi_0}{dx} + \frac{\partial \delta\psi}{\partial x}\right) + \frac{1}{S}\left(\frac{\partial^2\overline{\psi}_1}{\partial x^2} - k^2\overline{\psi}_1\right) - \frac{1}{R}\left(\frac{\partial^4\overline{\psi}_1}{\partial x^4} - 2k^2\frac{\partial^2\overline{\psi}_1}{\partial x^2} + k^4\overline{\psi}_1\right) \tag{12}$$

$$\frac{\partial}{\partial t}\left(\frac{\partial^2\overline{\phi}_1}{\partial x^2} - k^2\overline{\phi}_1\right) = k\left(\frac{d\psi_0}{dx} + \frac{\partial\delta\psi}{\partial x}\right)\left(\frac{\partial^2\overline{\psi}_1}{\partial x^2} - k^2\overline{\psi}_1\right) - k\left(\frac{d^3\psi_0}{dx^3} + \frac{\partial^3\delta\psi}{\partial x^3}\right)\overline{\psi}_1. \tag{13}$$

Equations (11)-(13) are solved as an initial value problem — E' is chosen such that the equilibrium does not dissipate due to resistivity and viscosity.

For the magnetic field, we employ the configuration used in Ref. [10],

$$B_{0y}(x) = 1 - (1 + B_c)\mathrm{sech}(\zeta x), \tag{14}$$

where

$$\zeta x_s = \mathrm{sech}^{-1}\left[\frac{1}{(1+B_c)}\right]. \tag{15}$$

The constant B_c is chosen such that $B'_{0y}(x_s) = \pi/2$. We do not need to specify $B_{0z}(x)$ and $P_0(x)$ since incompressible equations are used. The resistivity and the viscosity are both

assumed to be constant. The initial conditions for $\overline{\psi}_1$ and $\overline{\phi}_1$ are the linear eigenfunctions multiplied with a small number and $\delta\psi(t=0)=0$ [10]. The boundary conditions are $\delta\psi(x)=\partial\delta\psi/\partial x=0$, and the values provided by the initial conditions such as $\overline{\psi}_1(x)=0,\ \overline{\phi}_1(x)=\partial\overline{\phi}_1/\partial x=0$ for $x=\pm x_w$. The chosen parameters are $k=0.25,\ R=10^5,\ S=9.4\times10^5,\ B_c=0.233509,\ \zeta=2.68298$ corresponding to two rational surfaces at $x=x_s=\pm0.25$. The results are checked to be independent of x_w, the grid size and the time-step.

The effective growth rate $\gamma=\partial\ln B_y(0)/\partial t$ versus time is shown in Fig. 1. The run was stopped at $\gamma=0$. For initial times, $t\lesssim 30$, $\gamma\sim0.04$ approximates the linear growth rate [10]. After that, the quasilinear effects begin to suppress the effective growth rate — γ decreases with time and reaches zero at $t\simeq 78$.

The magnetic energy

$$E_m=\frac{1}{8\pi}\int(B_x^2+B_y^2)dxdy=\frac{1}{8\pi}\int\left[(k\overline{\psi}_1\sin ky)^2+\left(\frac{\partial\psi}{\partial x}\right)^2\right]dxdy, \tag{16}$$

and the kinetic energy

$$E_k=\frac{1}{2}\rho\int(v_x^2+v_y^2)dxdy=\frac{1}{8\pi}\int\left[(k\overline{\phi}_1\cos ky)^2+\left(\frac{\partial\overline{\phi}_1}{\partial x}\sin ky\right)^2\right]dxdy, \tag{17}$$

as functions of time are given in Fig. 2. Here, the magnetic field is normalized to $B_{0y}(\pm\infty)$, while in the final expression of E_k the velocities are measured in units of the poloidal Alfvén velocity. It is clearly shown that the magnetic energy released in the reconnection process, following the development of the tearing mode, converts to kinetic energy and can drive large flows.

The contours for (a) $\psi_0+\overline{\psi}_1\cos ky$ and (b) $\psi_0+\overline{\psi}_1\cos ky+\delta\psi$ at the end of the run are given in Fig. 3. The flux surfaces in Fig. 3(a) resemble those for resistivity double tearing mode while those in Fig. 3(b) look different [11]. Equal time profiles for $\overline{\psi}_1(x)$ and $\delta\psi(x)$ are given in Fig. 3(c) and (d). Taking ψ_0 from Eq. (14) into account, the differences between Fig. 3(a) and (b) are not difficult to understand.

In Fig. 4, the profiles of (a) $\overline{v}_y=\partial\overline{\phi}_1/\partial x$, (b) $\partial\overline{v}_y/\partial x=-\partial^2\overline{\phi}_1/\partial x^2$, and (c) $\overline{B}_x=k\overline{\psi}_1$ contemporaneous with Fig. 3 are presented. Two very important points emerge: 1) the amplitude of the poloidal velocity $\overline{v}_y$ reaches the level required by the condition for ITB formation [8], and 2) the flow $\overline{v}_y$ and flow shear $\partial\overline{v}_y/\partial x$ remain at noticeable levels for $x\gtrsim 0.5$ where $\overline{B}_x$ is negligibly small. One cannot overemphasize the significance of the

latter finding; because the velocity shear layers are formed outside the magnetic islands on both sides, the (magnetic) turbulence may be suppressed and ITBs may form in these layers.

ITBs are generally accompanied by a strong $\boldsymbol{E} \times \boldsymbol{B}$

shear flow, low or negative magnetic shear, and turbulence suppression. It has been pointed out that $\boldsymbol{E} \times \boldsymbol{B}$ shear flow may be generated by a variety of mechanisms [3]. In positive magnetic shear discharges, for instance, it is the coupling of an internal mode with an external MHD mode that leads to the local braking of the toroidal and poloidal rotations and then the $\boldsymbol{E} \times \boldsymbol{B}$ sheared flow results. This mechanism does not seem to work in discharges with central negative shear. The very stimulating observation that may provide supporting evidence for the mechanism proposed in this work is that two radially separated ITBs simultaneously exist and follow the two $q = 2$ surfaces in a section of JET discharge pulse 51573 [9]. Moreover, it is confirmed that the ITBs are terminated by an $m = 2$ MHD mode which extends from the inner to the outer foot point location of the two ITBs. This is precisely the defining theoretical characteristic of the proposed double tearing mode.

The ITB emergence is sensitive to local conditions and, in particular, to the properties of the integral q surfaces with regard to MHD instabilities and other phenomena. Our initial results, though by no means a final explanation for experimental observations, are highly encouraging as they stand up to the test of a quantitative comparison with experiment. It is very likely that additional experimental and theoretical investigations in this direction will help to expose the ITB triggering mechanism.

Finally, we would like to make an estimate for the fluid dynamic Reynolds number R, and generated velocity V_y. From $R = \tau_v/\tau_h$, $\tau_v = 4\pi a^4 n_e e^2/c^2\mu_e m_e = \omega_{pe}^2 a^4/c^2\mu_e$, and $\tau_h = a/v_A$, we have

$$R = \frac{\omega_{pe}^2 a^3 v_A}{c^2\mu_e} = 7.7 \times 10^{12} \frac{a^3 B\sqrt{n_e}}{\mu_e\sqrt{A}},$$

for n_e in $10^{20}/\mathrm{m}^3$, B in Tesla, a in meter, and μ_e in m^2/s. For typical tokamak discharge parameters $n_e = 0.1,\ B = .2$, we get

$$R = 10^{11} \frac{5a^3}{\mu_e\sqrt{A}}.$$

Lacking direct experimental observations on electron viscosity, and guided by the observed relations between ion viscosity and thermal diffusivity, we postulate it to be of the same order of magnitude as the electron thermal diffusivity. [12,13] Therefore, it is reasonable to estimate that $R \sim 5 \times 10^7$ for $a \sim 0.1,\ A = 1$ and $\mu_e \sim 10$.

The estimated viscous current penetration time (over a plasma sheet of width 0.1m) $\tau_v = \omega_{pe}^2 a^4/c^2\mu_e \sim 3.5$s for $n_e = 10^{19}\mathrm{m}^{-3}$ and $\mu_e = 10\mathrm{m}^2/\mathrm{s}$, then, does not contradict the experiment evidence [7].

For the viscosity double tearing modes, it is easy to estimate that the saturated poloidal shearing velocity

$$V_y \sim \frac{2^{4/15} B_{0y}'^{4/5} v_A}{(Rk)^{1/5}} \sim 0.1 v_A \sim 0.1 v_{ti},$$

for $R \sim 5 \times 10^7$ and $k = 0.1$ [10]. The scaling of the generated velocity with plasma parameters may be written as,

$$V_y \propto \frac{\mu_e^{4/5} B_{0y}'^{4/5}}{k^{1/5} n_e^{3/5} A^{2/5}}.$$

The fully nonlinear development of the mode is under investigation. Although the scaling with A and k seems in line with the experimental observations [3], the relation between the mode behavior and the minimum input NBI and RF power is a challenge for the model. **Possible directions to explore are: (1) macroscopic and microscopic electromagnetic perturbations that develop and cause anomalous electron viscosity do so only when the auxiliary heating power exceeds the threshold; (2) existence of a "proper" magnitude of viscosity that does allow the double tearing to develop (and the velocity shear layer to form) but does not allow the double tearing mode to develop too fast creating violent MHD activity. The threshold depends on the competition between $\boldsymbol{E} \times \boldsymbol{B}$ stabilization and the force that drives turbulence through instabilities like the ion and electron temperature gradient (ITG and ETG) modes and the trapped electron (TE) modes. The fact that the required threshold power in plasmas with reversed magnetic shear is lower than that with positive shear is attributed to the stabilization of the ballooning instability, larger Shafranov shift and lower safety factor near the magnetic axis [7]. In addition, the $\boldsymbol{E} \times \boldsymbol{B}$ velocity shear required to completely suppress the (ITG) modes in the former is lower than that in the latter [14].**

There is a common refrain in the literature that ITBs occur under various conditions depending on the interplay between the mechanisms that drive and suppress plasma turbulence. It is quite natural to expect that the mechanism proposed in this work is relevant only in plasmas with non-monotonic q profiles. Other mechanisms such as fishbone instability, mode coupling etc. could be

relevant elsewhere [7]. It is even possible that the resonance mechanism does not play a major role under certain conditions. At this stage there is no unique or universal mechanism

The electron viscosity mediated double tearing mode is shown to generate localized shear flows in plasma configurations with non-monotonic safety factor. The proposed mechanism emerges as a major contender for an ITB trigger because the generated shear flows bear such striking qualitative and quantitative similarity to the flows that accompany ITB formation (located in the proximity of low order rational surfaces, and just outside the magnetic islands).

Acknowledgments

One of the authors (JQD) acknowledges academician Li, ZhengWu for continuous encouragements and Prof. W. Horton for very helpful discussions. This work is supported by the National Natural Science Foundation of China, Grant No.10135020 and by U.S. Department of Energy, Grant No. DE-FG03-96ER-54346.

References

1. Y. Koide, M. Kikuchi, M. Mori, S. Tsuji, S. Ishida *et al.*, Phys. Rev. Lett. **72**, 3662 (1994).

2. C.M. Greenfield, C.L. Rettig, G.M. Staebler *et al. International Atomic Energy Agency, 1998*, p. 413.

3. M.G. Bell, R.E. Bell, P.C. Efthimon, *et al.*, Plasma Phys. Control. Fusion **41**, A719 (1999).

4. G.M.D. Hogeweij, Y. Baranov, G.D. Conway, *et al.*, Plasma Phys. Control. Fusion **44**, 1155 (2002).

5. S. Gunter, G.D. Conway, A. Gude, J. Hobirk, M. Marasccek, A.G. Peeters, R.C. Wolf, and the ASDEX Upgrade Team, *28th EPS Conference on Controlled Fusion and Plasma Physics, June 18-22, 2001*, Paper P1.006.

6. E. Joffrin, C.D. Charlis, T.C. Hender, D.F. Howell, and G.T.A. Huysmans, Nucl. Fusion **42**, 235 (2002).

7. R.C. Wolf, Plasma Phys. Control. Fusion **45**, R1 (2003).

8. S.M. Mahajan and Z. Yoshida, Phys. Plasmas **7**, 635 (2000).

9. E. Joffrin, G. Gorini, C.D. Charlis, N.C. Hawkes, T.C. Hender, D.F. Howell, P. Maget, D. Mazon, S.E. Sharapov, G. Tresset, and contributors to the EFDA-JET Work Programme, Plasma Phys. Control, Fusion **44**, 1739 (2002).

10. J. Q. Dong, S.M. Mahajan, and W. Horton, Phys. Plasmas **10**, 3151 (2003).

11. D. Schnack and J. Killeen, in *Theoretical and Computational Plasma Physics* (International Atomic Energy Agency, Vienna, 1978), p. 337.

12. K. H. Burrell, R. J. Groebner, H. St. John, and R. P. Seraydarian, Nucl. Fusion **28**, 3 (1988).

13. S. D. Scott, M. Bitter, and R. J. Fonker, *et al.*, IAEA-CN-50/E-III-5, p. 655.

14. J. Q. Dong and W. Horton, Phys. Fluids **B 5**, 1581 (1993).

Figure Captions

1. The effective growth rate $\gamma = \partial \ln B_y(0)/\partial t$ versus time.

2. The kinetic energy E_k (a) and magnetic energy E_m (b) versus time.

3. The contours for (a) $\psi_0 + \overline{\psi}_1 \cos ky$ and (b) $\psi_0 + \overline{\psi}_1 \cos ky + \delta\psi$. The profiles of (c) $\overline{\psi}_1(x)$ and (d) $\delta\psi(x)$.

4. The profiles of (a) $\overline{v}_y$, (b) $\partial \overline{v}_y/\partial x$, and (c) $\overline{B}_x$.

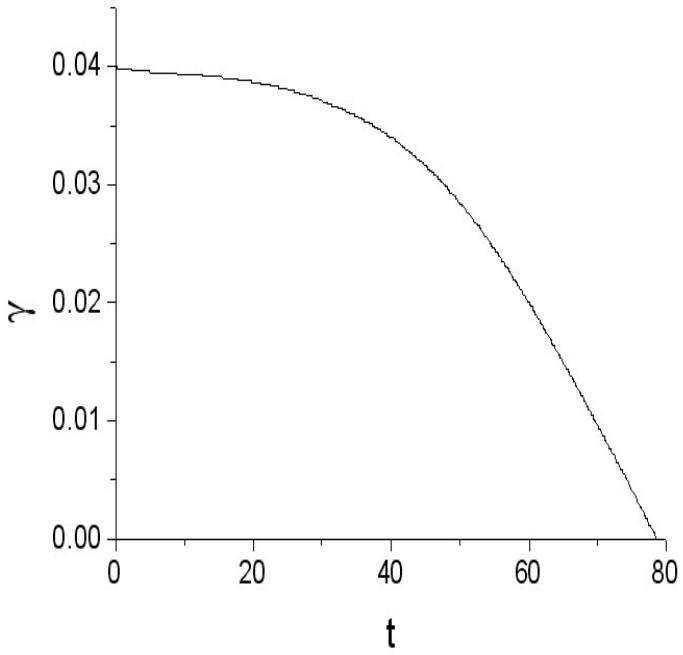

FIG. 1:

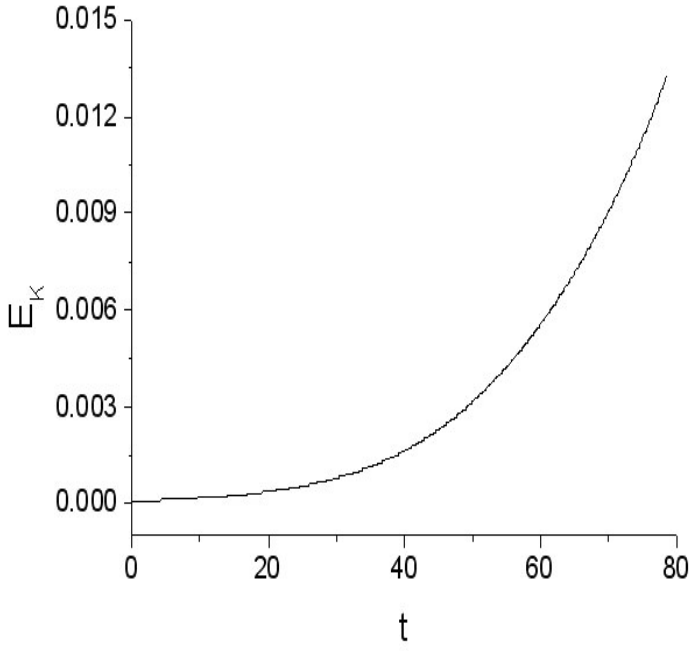

FIG. 2a:

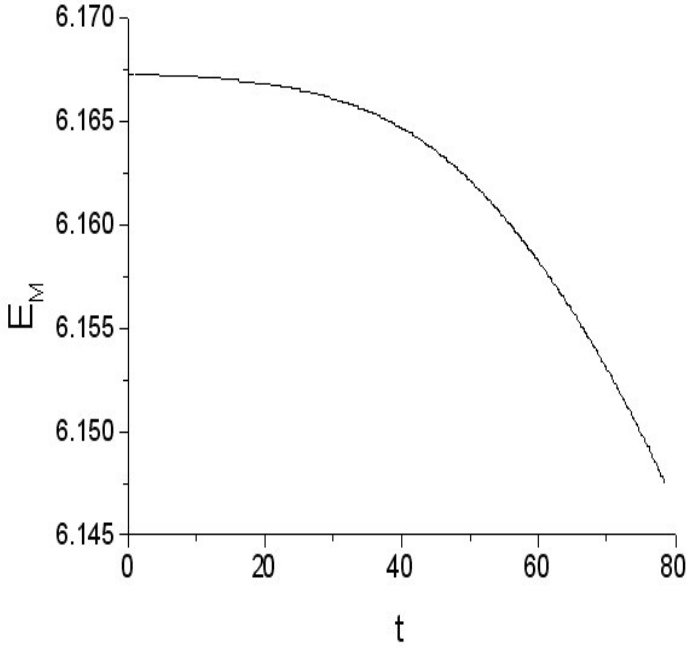

FIG. 2b:

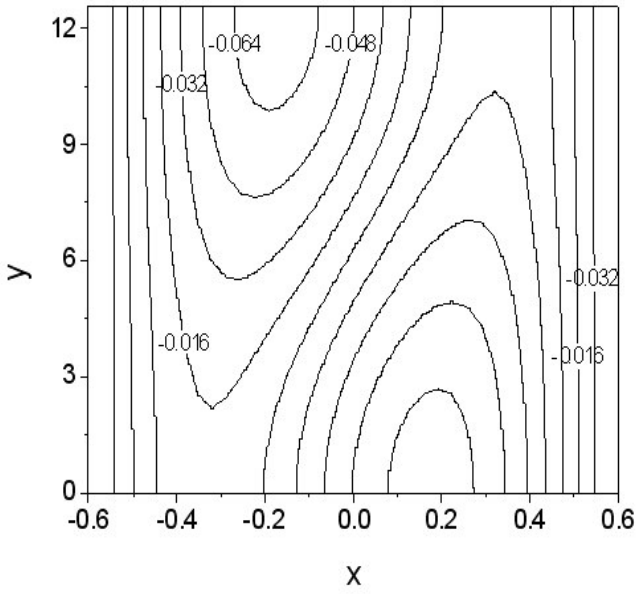

FIG. 3a:

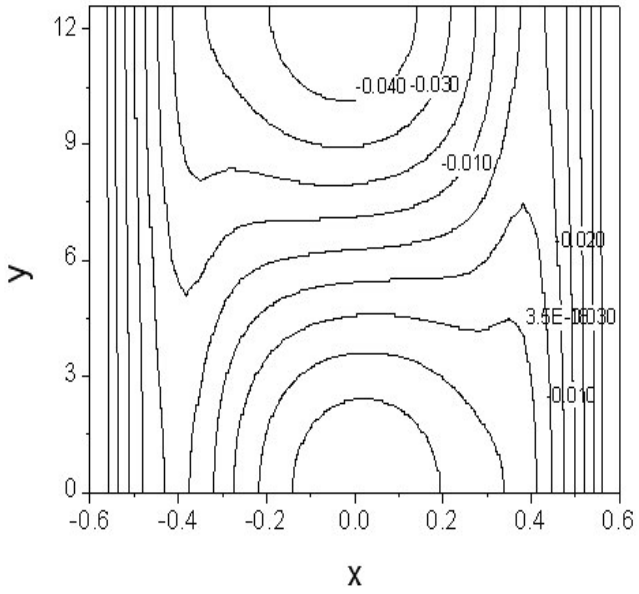
12
9
6
3
0
y
-0.6
-0.4
-0.2
0.0
0.2
0.4
0.6
x
-0.040
-0.030
-0.010
-0.020
3.5E-16030
-0.010

FIG. 3b:

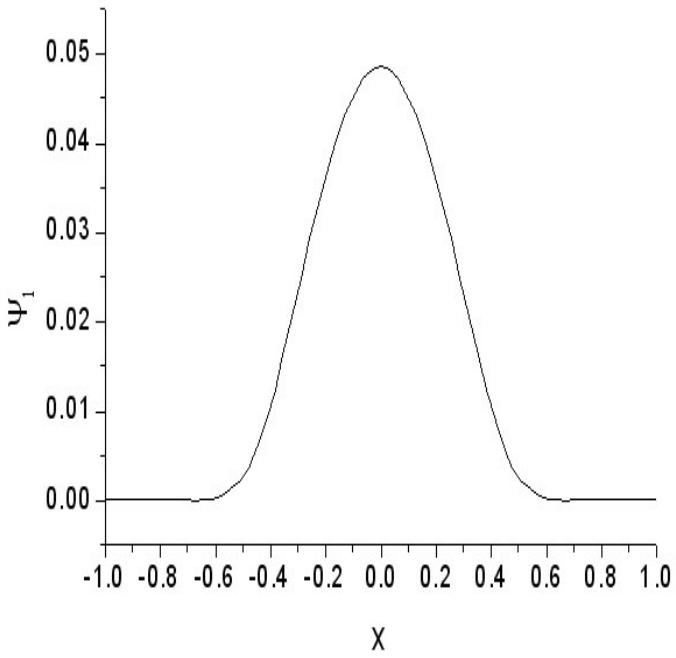

FIG. 3c:

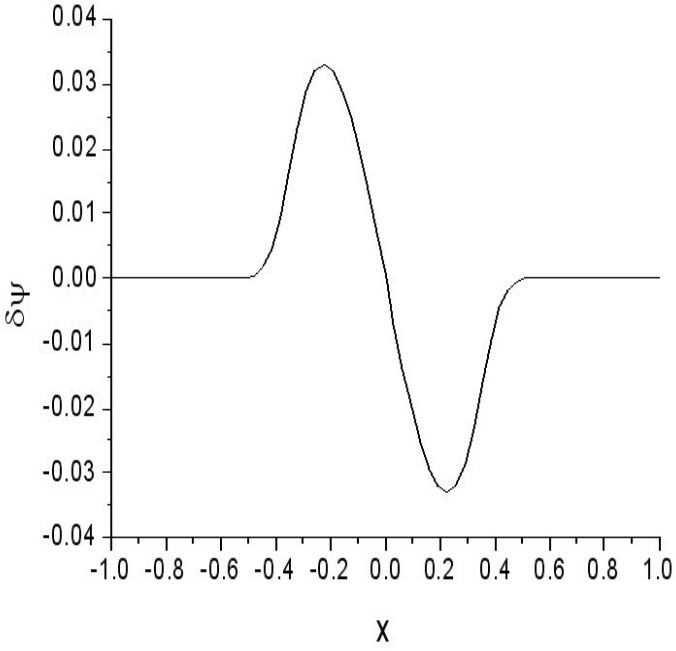
0.04
0.03
0.02
0.01
0.00
-0.01
-0.02
-0.03
-0.04
δψ
-1.0 -0.8 -0.6 -0.4 -0.2 0.0 0.2 0.4 0.6 0.8 1.0
X

FIG. 3d:

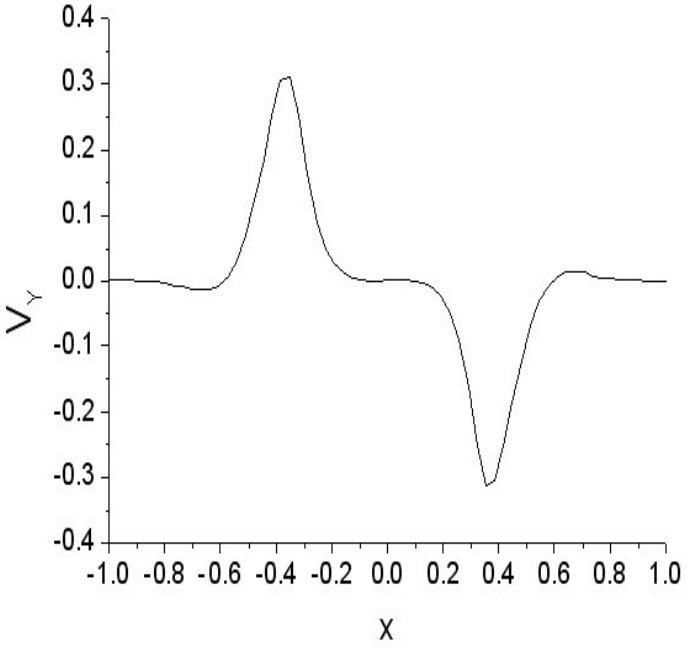

FIG. 4a:

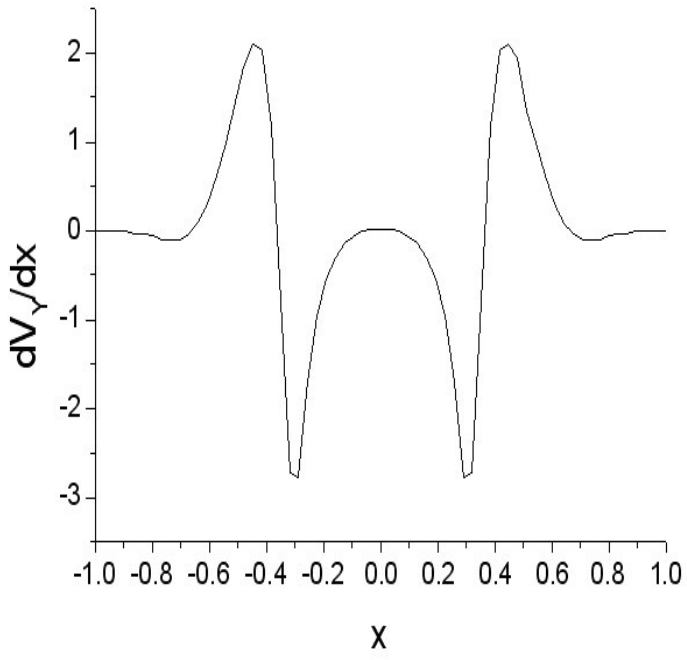

FIG. 4b:

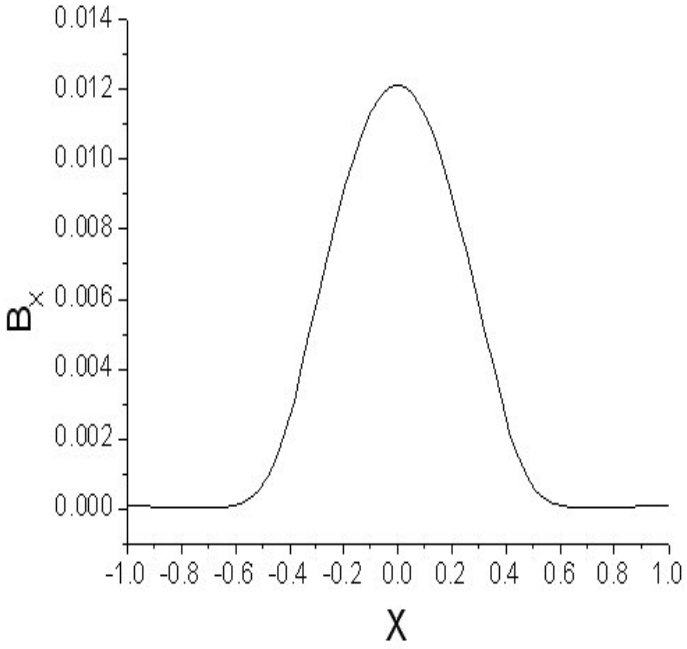
0.014
0.012
0.010
0.008
0.006
0.004
0.002
0.000
B_x
-1.0 -0.8 -0.6 -0.4 -0.2 0.0 0.2 0.4 0.6 0.8 1.0
X

FIG. 4c: